CORE
Metadata, citation and similar papers at core.ac.uk
Provided by NASA Technical Reports Server

121097
P-24

NASA Technical Memorandum

NASA TM - 103602

THE EFFECT OF WELD POROSITY ON THE CRYOGENIC FATIGUE STRENGTH OF ELI GRADE Ti-5Al-2.5Sn

By P.R. Rogers, R.C. Lambdin, and D.E. Fox

Materials and Processes Laboratory
Science and Engineering Directorate

September 1992

(NASA-TM-103602) THE EFFECT OF WELD POROSITY ON THE CRYOGENIC FATIGUE STRENGTH OF ELI GRADE Ti-5Al-2.5Sn (NASA) 24 p

N92-33603

Unclas

G3/26 0121097

National Aeronautics and
Space Administration

George C. Marshall Space Flight Center

MSFC - Form 3190 (Rev. May 1983)

REPORT DOCUMENTATION PAGE

Form Approved
OMB No. 0704-0188

Public reporting burden for this collection of information is estimated to average 1 hour per response, including the time for reviewing instructions, searching existing data sources, gathering and maintaining the data needed, and completing and reviewing the collection of information. Send comments regarding this burden estimate or any other aspect of this collection of information, including suggestions for reducing this burden, to Washington Headquarters Services, Directorate for Information Operations and Reports, 1215 Jefferson Davis Highway, Suite 1204, Arlington, VA 22202-4302, and to the Office of Management and Budget, Paperwork Reduction Project (0704-0188), Washington, DC 20503.

1. AGENCY USE ONLY *(Leave blank)*

2. REPORT DATE
September 1992

3. REPORT TYPE AND DATES COVERED
Technical Memorandum

4. TITLE AND SUBTITLE
The Effect of Weld Porosity on the Cryogenic Fatigue Strength of ELI Grade Ti-5Al-2.5Sn

5. FUNDING NUMBERS

6. AUTHOR(S)
P.R. Rogers, R.C. Lambdin, and D.E. Fox

7. PERFORMING ORGANIZATION NAME(S) AND ADDRESS(ES)
George C. Marshall Space Flight Center
Marshall Space Flight Center, Alabama 35812

8. PERFORMING ORGANIZATION REPORT NUMBER

9. SPONSORING/MONITORING AGENCY NAME(S) AND ADDRESS(ES)
National Aeronautics and Space Administration
Washington, DC 20546

10. SPONSORING/MONITORING AGENCY REPORT NUMBER
NASA TM - 103602

11. SUPPLEMENTARY NOTES
Prepared by Materials and Processes Laboratory, Science and Engineering Directorate

12a. DISTRIBUTION/AVAILABILITY STATEMENT
Unclassified-Unlimited

12b. DISTRIBUTION CODE

13. ABSTRACT *(Maximum 200 words)*

The effect of weld porosity on the fatigue strength of ELI grade Ti-5Al-2.5Sn at cryogenic temperature was determined. A series of high cycle fatigue (HCF) and tensile tests were performed at -320 degrees F on specimens made from welded sheets of the material. All specimens were tested with weld beads intact and some amount of weld offset. Specimens containing porosity and control specimens containing no porosity were tested. Results indicate that for the weld configuration tested, the fatigue life of the material is not affected by the presence of spherical embedded pores.

14. SUBJECT TERMS
Titanium
Weld Porosity
Fatigue

15. NUMBER OF PAGES
25

16. PRICE CODE
NTIS

17. SECURITY CLASSIFICATION OF REPORT	18. SECURITY CLASSIFICATION OF THIS PAGE	19. SECURITY CLASSIFICATION OF ABSTRACT	20. LIMITATION OF ABSTRACT
Unclassified	Unclassified	Unclassified	

TABLE OF CONTENTS

PRECEDING PAGE BLANK NOT FILMED

LIST OF ILLUSTRATIONS

LIST OF TABLES

TECHNICAL MEMORANDUM

THE EFFECT OF WELD POROSITY ON THE CRYOGENIC FATIGUE STRENGTH OF ELI GRADE Ti-5Al-2.5Sn

INTRODUCTION

The purpose of this study was to determine the fatigue strength reducing effects of weld porosity for GTAW Ti-5Al-2.5Sn (ELI). Weld defects of this kind are encountered on space shuttle main engine high pressure fuel turbopump inlets which are made from welded sheets of this material and which operate at a temperature of –390 °F in an environment of liquid hydrogen.

Low-temperature high-cycle fatigue (NCF) and tensile tests were performed on dog-bone specimens made from welded sheets. An attempt was made to test welds typical of those found in flight hardware at conditions similar to those encountered in flight. The effect of porosity on the fatigue strength of the material was determined by comparing test results for specimens containing porosity with results for control specimens containing no porosity and with existing HCF data for the material.

EQUIPMENT

The HCF and tensile tests were performed using the MTS 20 kip test system, which is shown in figure 1. To obtain the required steady-state temperature, the specimens were completely immersed in liquid nitrogen, which was maintained at a constant level by a system of thermocouples and relays.

TEST SPECIMENS

There were 31 dog-bone test specimens machined with weld beads intact from 7 sheets of stress-relieved GTAW Ti-5Al-2.5Sn. The specimen geometry is depicted in figure 2. The weld bead was completely contained within the straight section shown in the middle of the specimen. Welders intentionally produced varying amounts of porosity in six of the seven panels, and x rays were used to establish the size and distribution of pores in the panels and in the machined specimens. Five specimens were obtained from the panel with no porosity, and 26 specimens were machined from the panels with weld porosity. Table 1 [1] lists the size and number of pores for the 21 valid HCF test specimens which contained pores. Weld offset varied among specimens, ranging from 1.7 to 48 percent. Further information on specimen geometry can be found in table 2.

Metallography showed nominal microstructure and grain sizes ranging from ASTM No. 8 in the parent metal to ASTM No. 1 in the weld. Representative micrographs are shown in figure 3. The heat-affected zone extended approximately 0.125 inches beyond the weld interface. Microhardness readings showed a hardness of R_c 28 throughout the specimen.

TESTING

The specimens were mounted in the test fixture shown in figure 4, and the complete assembly was mounted into the cryostat and brought to a steady-state temperature of –320 °F. Testing was performed under load control at a sinusoidal frequency of 50 Hz. Twenty-three HCF tests were performed at –320 °F on specimens containing porosity, and five NCF tests were performed at –320 °F on specimens without porosity. The specimens were tested at high R-ratios, since this is typical of conditions encountered in flight hardware. The remaining three specimens were tested at –320 °F to determine the tensile properties.

RESULTS AND DISCUSSION

The results of the HCF tests are shown in figures 5 and 6 and in table 3. The bending stress induced by weld offset is accounted for in the "corrected" stress plotted in figure 5, while figure 6 shows the data before correcting for weld offset. Fatigue test results for GTAW wrought Ti-5Al-2.5Sn (also tested at –320 °F) are the basis of the S-N curve used to predict the fatigue life of welded of Ti-5Al-2.5Sn. A best fit line through data for these tests [2] is plotted for comparison in figures 5 and 6. Data corrected for offset tend to fall above this line, which indicates that the offset correction is conservative. A sample calculation of this treatment of offset is given in the appendix. All results were converted to $R = -1$ using the Goodman relationship, and this calculation is also described in the appendix. Data for the three tensile test specimens are listed in table 4.

Of 21 valid fatigue test specimens containing porosity, only five specimens failed through pores. Figures 5 and 6 show that there was no trend for the specimens which failed through pores to fail earlier than specimens which did not fail through pores. Figure 7 shows the pore sizes and locations for these specimens. Scanning electron microscope (SEM) and visual analysis revealed spherical pores with smooth internal surfaces. The pores did not act as initiation sites. The transgranular fractures initiated predominantly at the crown side of the weld interface and propagated through the heat affected zone. Representative factographs are shown in figure 8.

CONCLUSION

Embedded pores did not act as initiation sites for fatigue failures and did not cause a reduction in the fatigue life of the specimens tested. Thus, for this weld configuration, the fatigue life of Ti-5Al-2.5Sn is not affected by the presence of spherical embedded pores within the range of sizes tested. Other factors, such as weld offset and the notch effect of the weld bead, more strongly influence the fatigue life of the welded material.

ORIGINAL PAGE
BLACK AND WHITE PHOTOGRAPH

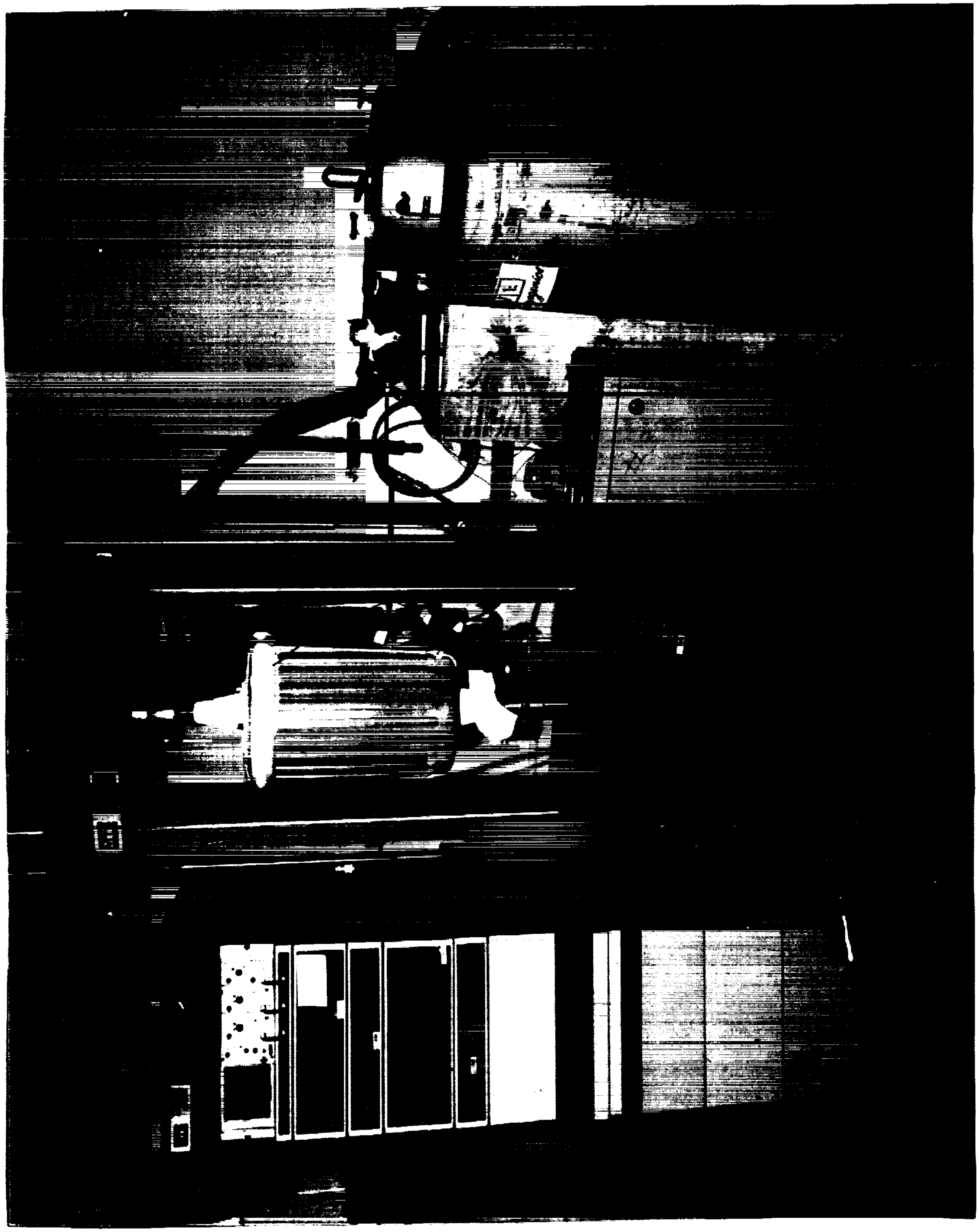

Figure 1. MTS test system.

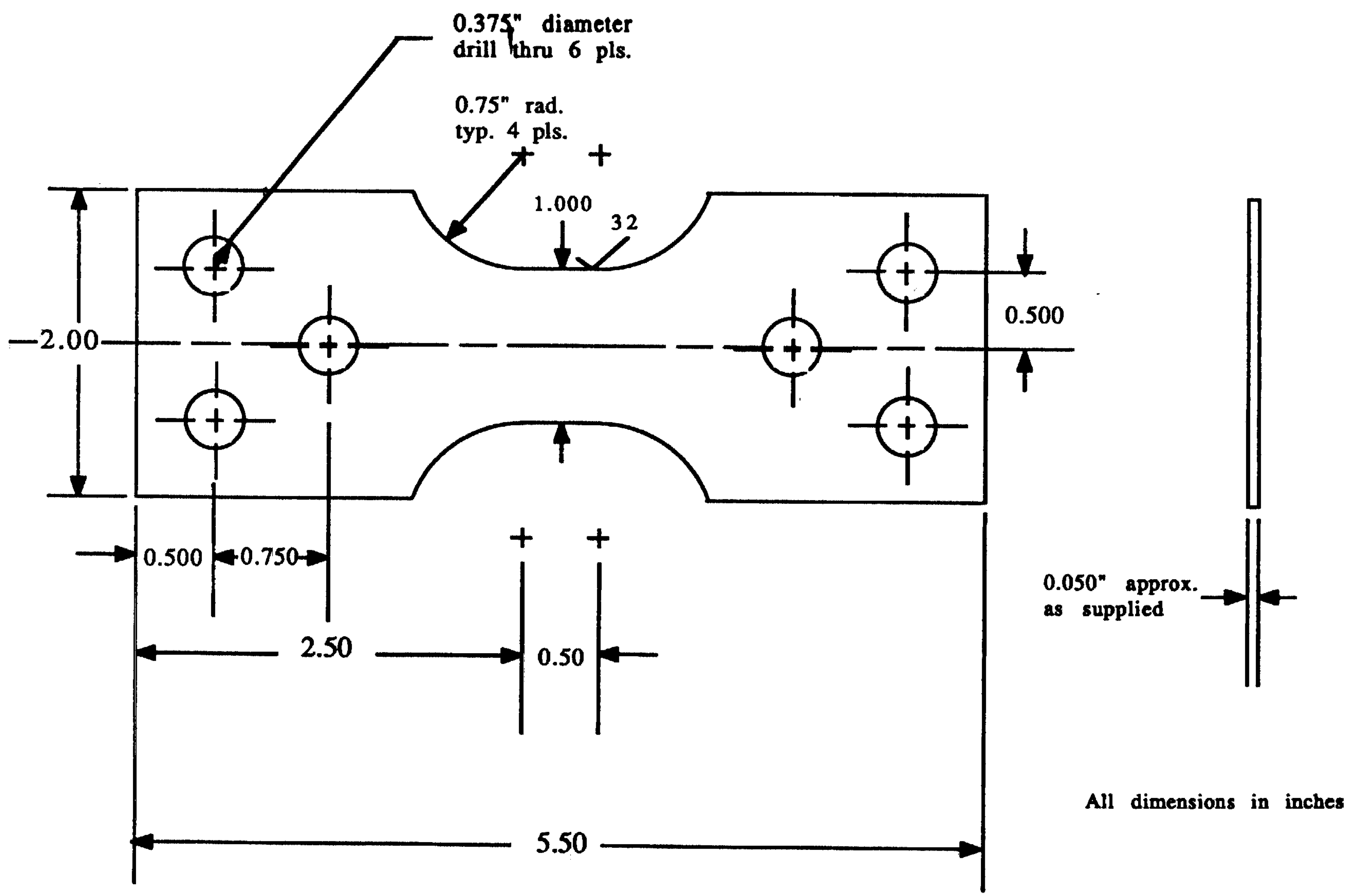

Figure 2. Specimen geometry.

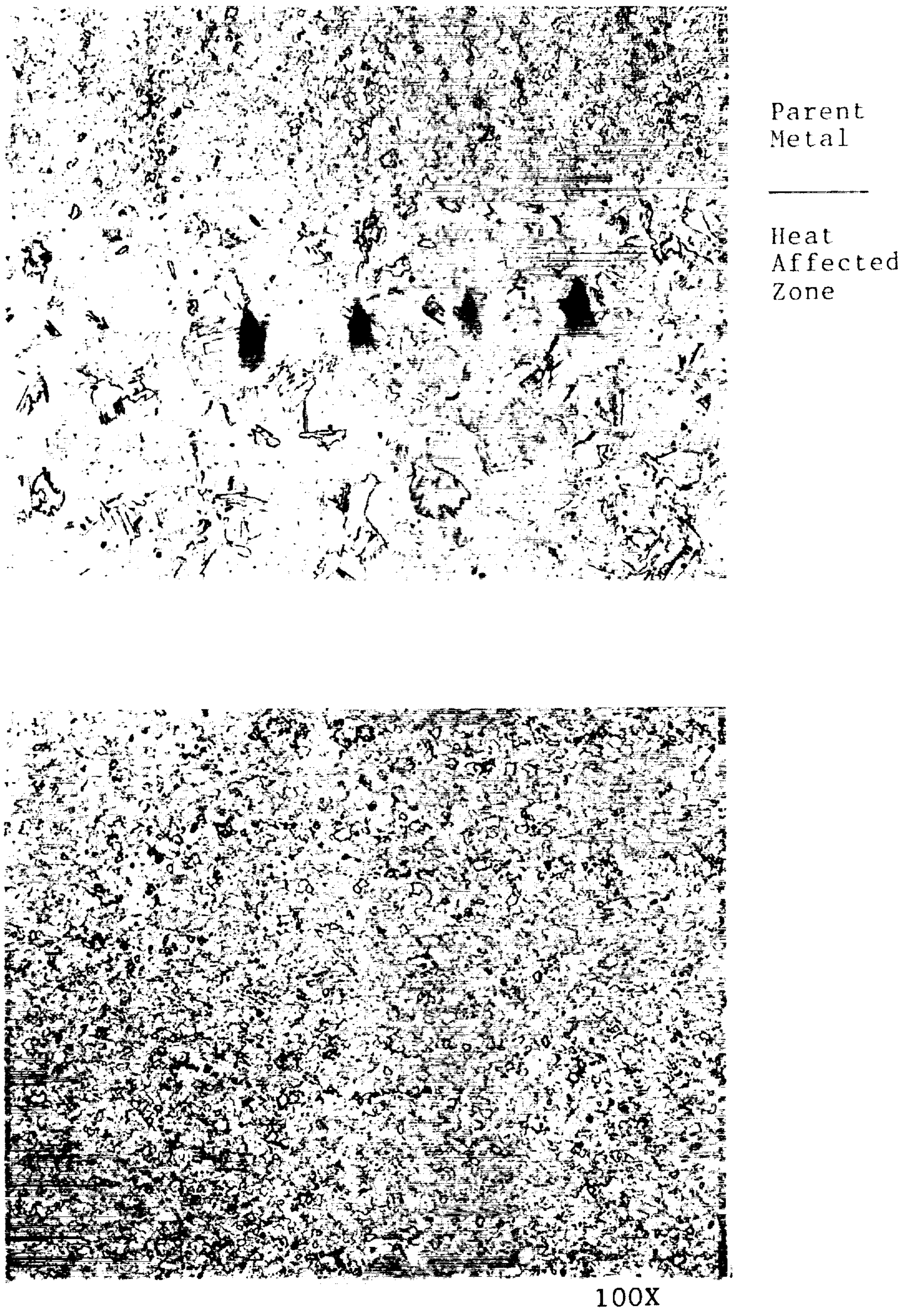

Figure 3. Representative microstructure.

ORIGINAL PAGE
BLACK AND WHITE PHOTOGRAPH

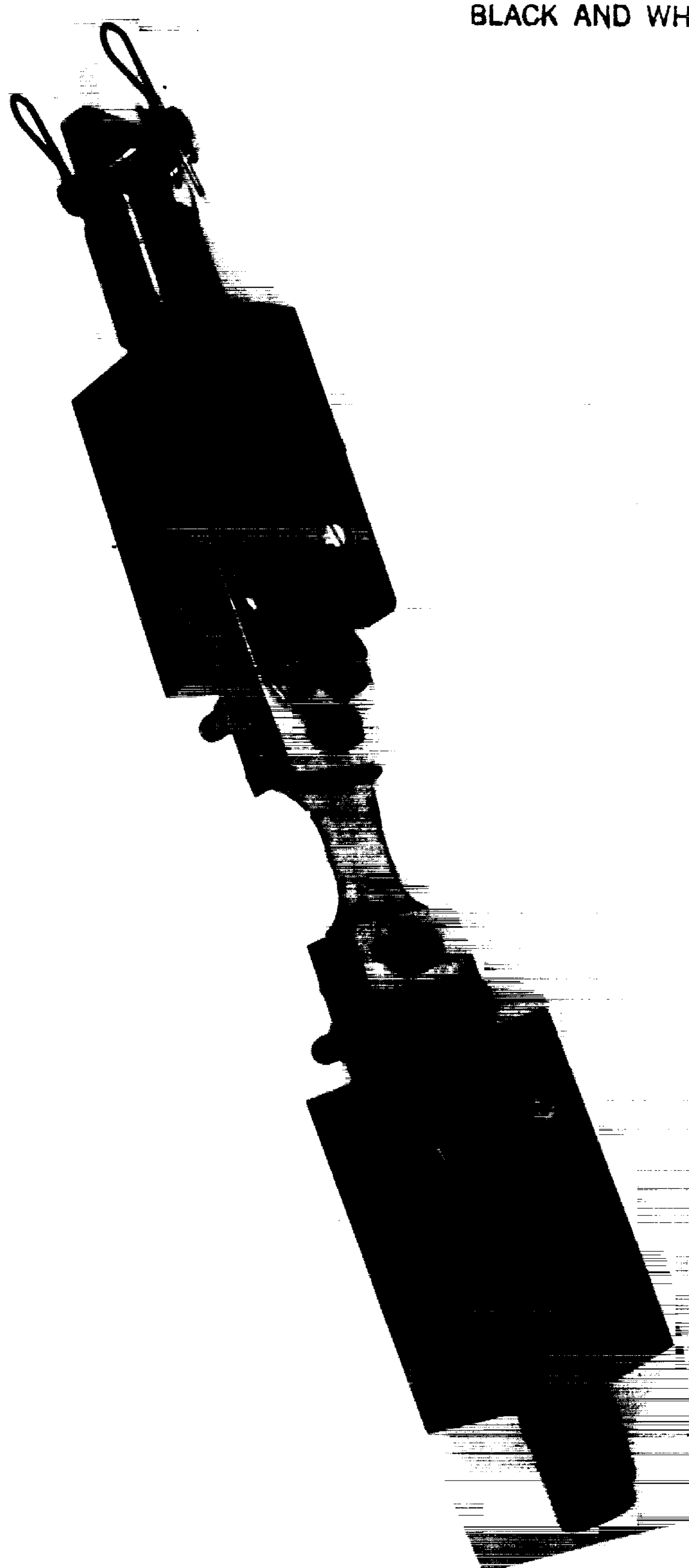

Figure 4. Test fixture.

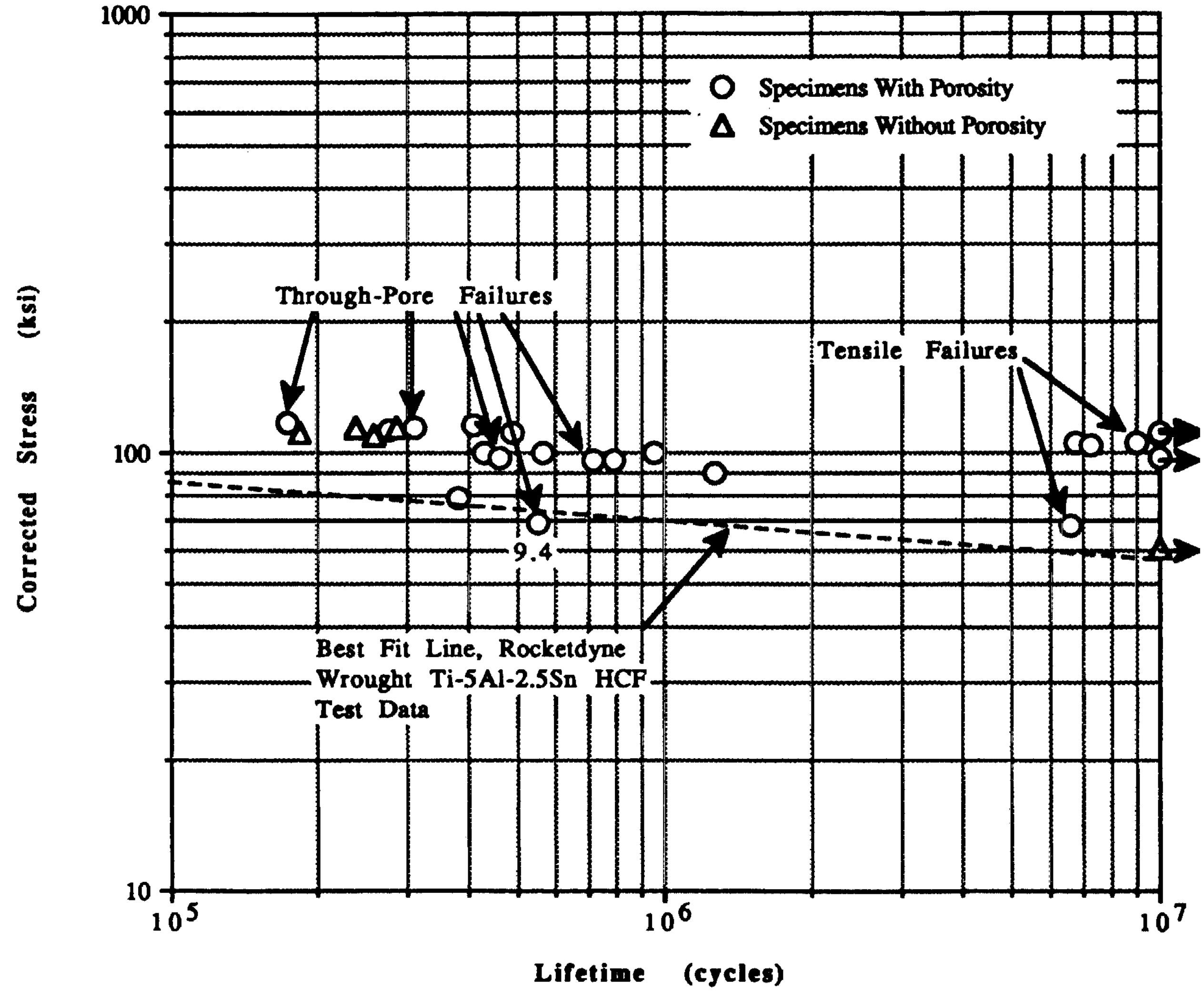

Figure 5. S-N plot, corrected stress.

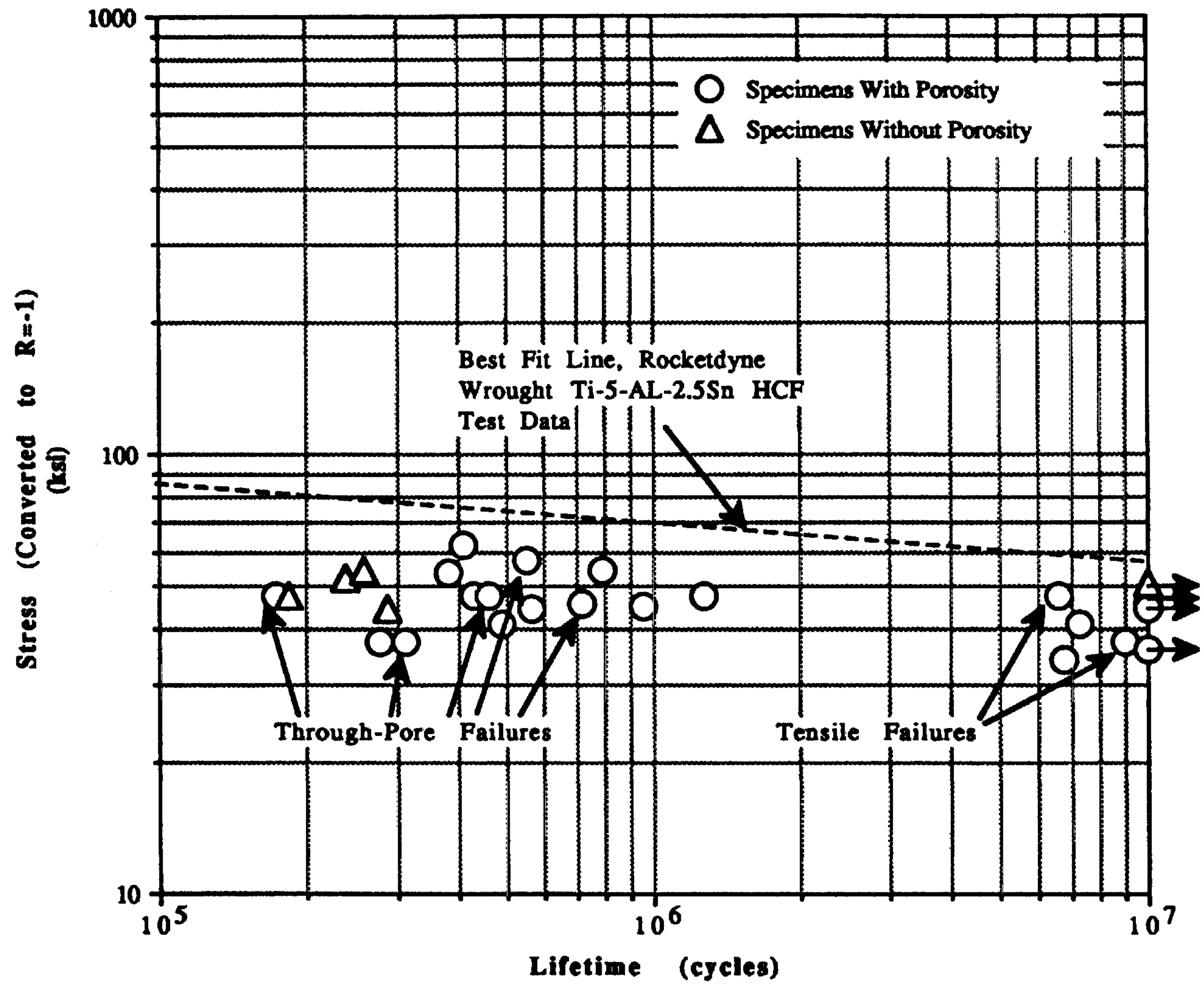

Figure 6. S-N plot, data not corrected for offset.

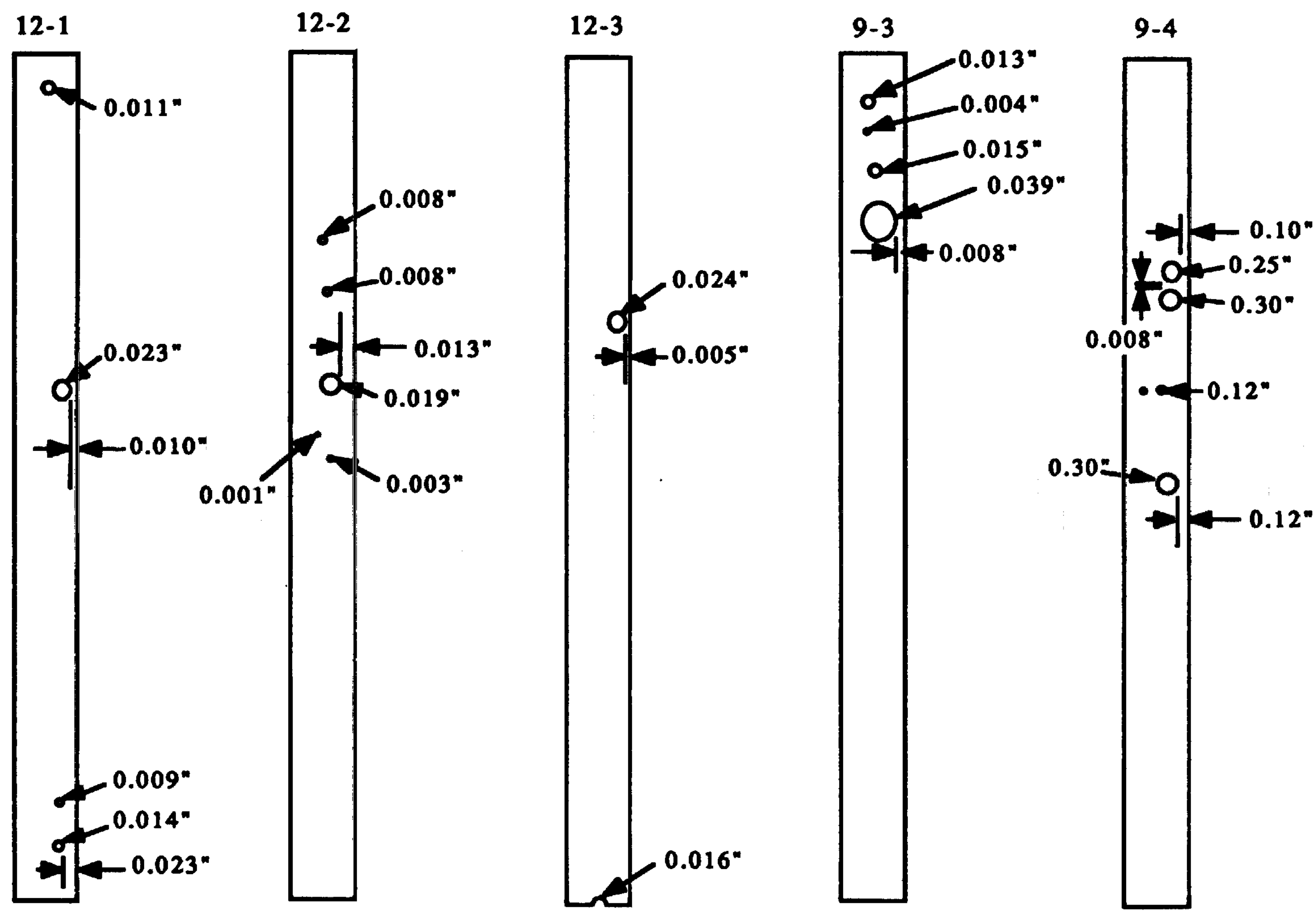

Figure 7. Pore sizes and locations in specimen cross sections.

ORIGINAL PAGE
BLACK AND WHITE PHOTOGRAPH

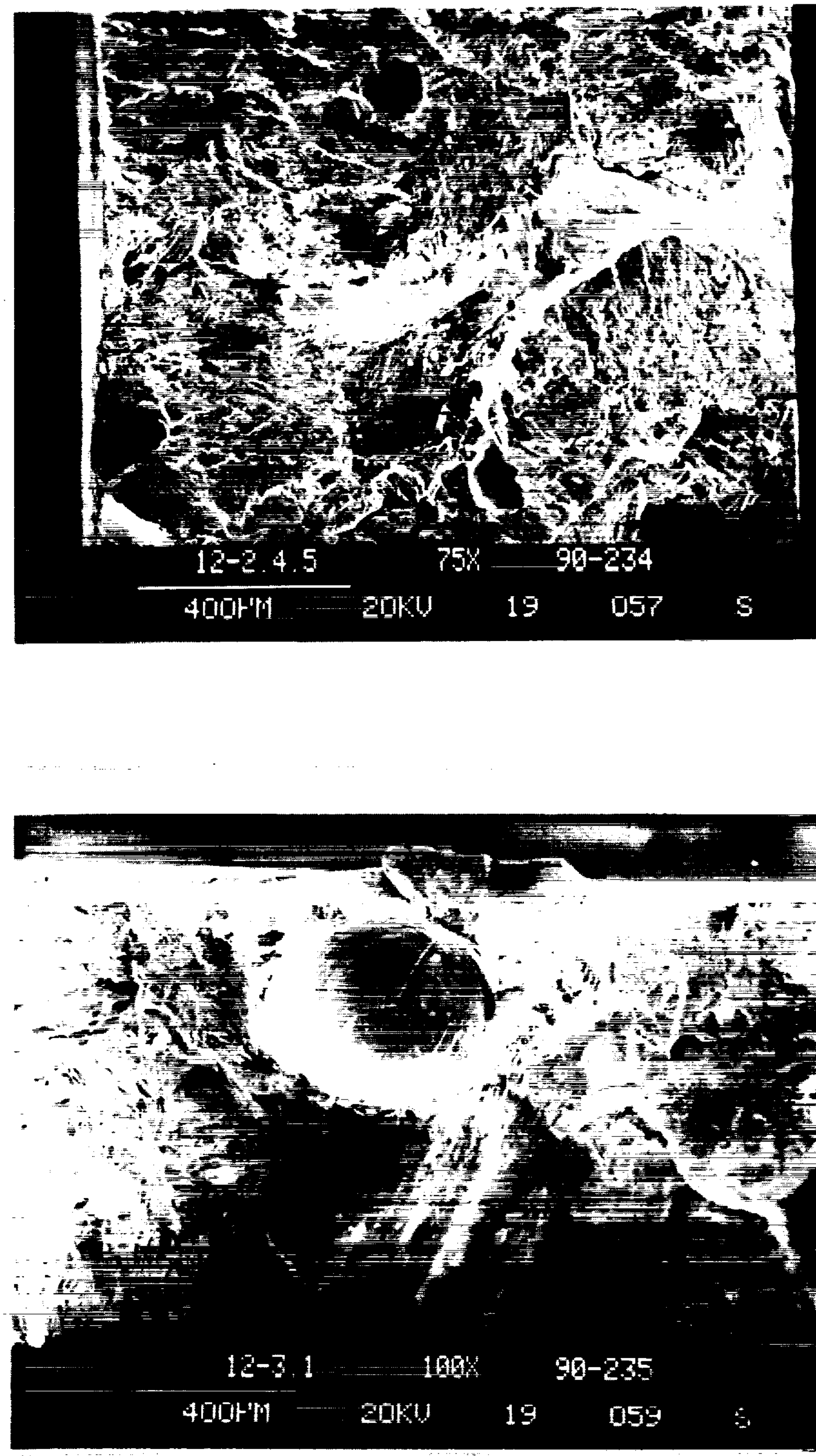

Figure 8. SEM photos of fracture surfaces showing typical pores.

Table 1. Porosity count, valid HCF test specimens.

	Pore Diameter (in.)											
	9.1	9.3	9.4	10.2	10.5	11.1	11.2	11.3	11.4	12.1	12.2	12.3
Pore 1	0.01	0.04	0.032	0.017	0.012	0.022	0.036	0.017	0.012	0.018	0.017	0.012
Pore 2	0.01	0.03	0.025	0.014	0.012	0.019	0.024	0.012	0.012	0.014	0.014	0.012
Pore 3	0.01	0.026	0.023	0.012	0.012	0.016	0.022	0.012	0.008	0.012	0.012	0.008
Pore 4	0.01	0.026	0.018	0.012	0.012	0.012	0.016	0.012	0.008	0.012	0.012	0.008
Pore 5	0.005	0.016	0.018	0.012	0.012	0.012	0.016	0.012	0.008	0.012	0.012	0.008
Pore 6	0.005	0.016	0.018	0.012	0.007	0.008	0.014	0.006	0.008	0.012	0.007	0.008
Pore 7	0.005	0.005	0.018	0.008	0.007	0.005	0.014	0.006	0.008	0.012	0.007	0.008
Pore 8	0.005	0.005	0.007	0.008	0.007	0.005	0.011	0.006	0.008	0.008	0.007	0.008
Pore 9	0.005		0.007	0.008	0.007	0.005	0.011	0.006	0.008	0.008	0.005	0.008
Pore 10			0.007	0.008	0.007	0.005	0.008	0.006	0.006	0.008		0.006
Pore 11			0.007	0.006	0.007	0.005	0.008	0.005	0.006	0.008		0.006
Pore 12			0.007	0.006	0.005		0.005	0.005	0.006	0.008		0.006
Pore 13			0.004	0.006	0.005		0.005	0.005	0.006	0.008		0.006
Pore 14			0.004	0.006	0.005				0.004	0.005		0.004
Pore 15				0.006					0.004	0.005		0.004
Pore 16									0.004	0.005		0.004
Pore 17									0.004			
Pore 18									0.004			
Pore 19									0.004			
Pore 20									0.004			
Total #	9	8	14	15	14	11	13	13	20	16	9	16
Max. Pore Size	0.01	0.04	0.032	0.017	0.012	0.022	0.036	0.017	0.012	0.018	0.017	0.012
Avg. Pore Size	0.007	0.02	0.014	0.01	0.008	0.01	0.015	0.008	0.007	0.01	0.01	0.007
Std.	0.003	0.012	0.009	0.003	0.003	0.006	0.009	0.004	0.003	0.004	0.004	0.003

(Pore diameter measurement accuracy = +/- 0.003")

Table 1. Porosity count, valid HCF test specimens (Continued)

	Pore Diameter (in.)								
	12.4	**13.1**	**13.3**	**13.4**	**14.1**	**14.2**	**14.3**	**14.4**	**14.5**
Pore 1	0.024	0.026	0.038	0.022	0.024	0.018	0.022	0.026	0.014
Pore 2	0.014	0.008	0.028	0.013	0.018	0.018	0.016	0.022	0.011
Pore 3	0.008	0.008	0.02	0.013	0.016	0.012	0.012	0.018	0.011
Pore 4	0.008	0.008	0.024	0.013	0.008	0.012	0.012	0.012	0.011
Pore 5	0.008	0.008	0.012	0.011	0.008	0.012	0.012	0.012	0.011
Pore 6	0.008	0.006	0.012	0.01	0.008	0.012	0.012	0.012	0.008
Pore 7	0.008	0.006	0.012	0.01	0.008	0.012	0.012	0.012	0.008
Pore 8	0.005		0.012	0.007	0.008	0.008	0.007	0.006	0.008
Pore 9	0.005		0.01	0.007	0.004	0.008	0.007	0.006	0.008
Pore 10	0.005		0.007	0.007	0.004	0.008	0.007	0.006	0.005
Pore 11	0.005		0.005	0.007	0.004	0.005	0.005		0.005
Pore 12			0.005	0.005	0.004	0.005	0.005		0.005
Pore 13			0.005	0.005	0.004	0.005	0.005		
Pore 14					0.004	0.005			
Pore 15						0.005			
Pore 16						0.005			
Pore 17						0.005			
Pore 18						0.005			
Pore 19						0.005			
Pore 20									
Total #	11	7	13	13	14	19	13	10	12
Max. Pore Size	0.024	0.026	0.038	0.022	0.024	0.018	0.022	0.026	0.014
Avg. Pore Size	0.009	0.01	0.015	0.01	0.009	0.009	0.01	0.013	0.009
Std.	0.006	0.007	0.01	0.005	0.006	0.005	0.005	0.007	0.003

(Pore diameter measurement accuracy = +/- 0.003")

Table 2. Specimen geometry data.

Specimen	Width (in.)	Thickness (in.)	Area (in.)	% Offset (-)	Peaking (deg.min)	Weld Thickness (in.)	Offset Correction Factor
9.1	0.999	0.058	0.058	3.4	1.54	0.0785	1.102
9.2	1.000	0.0589	0.0589	23.8	2.11	0.0807	N/A TENSION TEST
9.3	1.000	0.0592	0.0592	35	2.1	0.0839	2.05
9.4	1.000	0.0594	0.0594	1.7	1.23	0.0818	1.051
10.1	1.000	0.056	0.056	3.6	2.18	0.0747	1.107
10.2	1.000	0.0565	0.0565	28.3	2.56	0.0792	1.85
10.3	1.000	0.0563	0.0563	48	3.6	0.0775	N/A TENSION TEST
10.4	1.000	0.0569	0.0569	35.1	3.3	0.0768	N/A TENSION TEST
10.5	1.000	0.0575	0.0575	33.04	2.56	0.0745	1.99
11.1	0.999	0.0575	0.0574	7	2.46	0.0773	1.21
11.2	0.999	0.0579	0.0579	17.2	3.27	0.0762	1.516
11.3	1.000	0.0592	0.0592	30.4	2.4	0.0748	1.91
11.4	1.000	0.0593	0.0593	13.5	1.44	0.0834	1.405
12.1	1.000	0.0533	0.0533	13.2	2.8	0.0754	1.39
12.2	1.000	0.0525	0.0525	36.2	2.52	0.0782	2.1
12.3	0.998	0.0515	0.0514	13.6	1.44	0.0767	1.41
12.4	1.000	0.0498	0.0498	26.1	0.52	0.0761	1.783
13.1	1.000	0.0565	0.0565	15.9	2.8	0.0754	1.477
13.2	1.000	0.0567	0.0567	15.9	3.2	0.0809	1.477
13.3	1.001	0.0567	0.0567	15.9	2.8	0.0828	1.477
13.4	1.000	0.057	0.057	3.5	2.25	0.0828	1.105
14.1	1.000	0.0555	0.0555	10.8	2.42	0.0731	1.32
14.2	0.999	0.0564	0.0564	23	2.35	0.0809	1.69
14.3	1.000	0.0555	0.056	34.2	2.52	0.0828	2.03
14.4	0.999	0.0558	0.0558	28.7	1.44	0.0821	1.861
14.5	1.000	0.0578	0.0578	29.4	2.18	0.0758	1.882
15.1	0.999	0.0585	0.0585	32.5	2.8	0.0839	1.975
15.2	0.999	0.059	0.0589	28.8	2.35	0.0772	1.864
15.3	1.000	0.0585	0.0585	29.1	3.27	0.0817	1.873
15.4	1.000	0.0585	0.0585	23.9	3.27	0.0778	1.717
15.5	1.000	0.059	0.059	1.7	3.27	0.0763	1.051

Table 3. HCF test results.

Specimen	Mean Stress (ksi)	Alt. Stress (ksi)	Salt (R=-1) (ksi)	Corrected Stress (ksi)	Life (cycles)	Comments
9.1	141	15.7	53.9	78.5	384000	
9.2	NO DATA, TENSION TEST SPECIMEN					
9.3	136.1	15.12	47.8	116.6	173486	FAILURE THROUGH PORES
9.4	143.35	15.93	57	68.6	552841	FAILURE THROUGH PORES
10.1	137.9	15.32	49.9	72.5	6765461	NEAR BOLT HOLE FAILURE
10.2	120.9	13.43	34.2	105.7	6739758	
10.3	NO DATA, TENSION TEST SPECIMEN					
10.4	NO DATA, TENSION TEST SPECIMEN					
10.5	123.5	13.7	36.1	110.3	10000000	R/O, 25 MILLION CYCLES
11.1	136.1	15.12	47.8	90.5	1271000	
11.2	133.1	14.79	44.7	100.6	566577	
11.3	129.59	14.4	41.3	110.7	491975	
11.4	134.34	14.9	45.9	97.2	10000000	R/O
12.1	134.64	14.9	46.1	96.6	718297	FAILURE THROUGH PORES
12.2	125.6	13.9	37.7	113.6	313177	FAILURE THROUGH PORES
12.3	136.12	15.1	47.8	98.0	464190	FAILURE THROUGH PORES
12.4	125.6	13.95	37.8	105.8	8990000	TENSILE FAILURE
13.1	136.1	15.12	47.8	100.4	430000	
13.2	133.1	14.79	44.7	99.3	196926	BOLT HOLE FAILURE
13.3	133.1	14.97	45.2	99.9	957672	
13.4	136.1	15.12	47.8	68.1	6579310	TENSILE FAILURE
14.1	141.2	15.7	54.1	96.7	792305	
14.2	129.6	14.4	41.3	104.7	7264049	
14.3	125.6	13.95	37.8	112.2	276159	
14.4	147.02	16.33	62.5	115.6	410681	
14.5	133.1	14.79	44.7	111.3	10000000	R/O
15.1	133.1	14.79	44.7	113.7	286991	NO POROSITY
15.2	136.1	15.12	47.8	111.9	182300	NO POROSITY
15.3	140	15.56	52.5	113.6	238000	NO POROSITY
15.4	141.2	15.7	54.1	109.7	257500	NO POROSITY
15.5	138.8	15.4	50.9	60.4	10000000	R/O, NO POROSITY

Table 4. Specimen tensile test data.

Specimen	Ultimate Tensile Strength (ksi)	Yield Strength at 2% offset (ksi)	% Elongation (-)
9.2	205	178	5.7
10.3	190	180	2.1
10.4	203	174	6.4
Average	**199**	**177**	**4.7**

APPENDIX – SAMPLE CALCULATIONS

1. Offset Correction

The full theoretical stress-raising effect of weld offset can be found by drawing a free body diagram of the welded sheet. Fixed ends are assumed as shown in figure A-1 since rotation in the plane of the paper is prevented in the test setup.

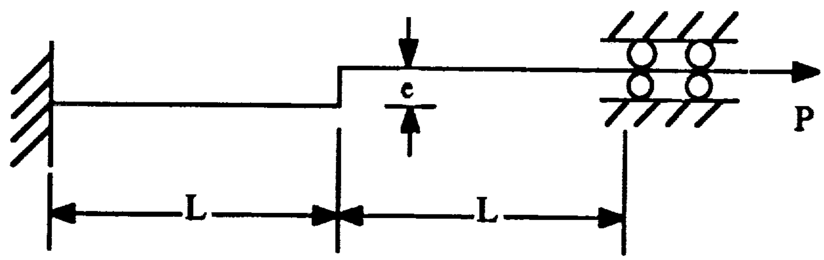

Figure A-1. The test setup.

The situation shown can be reduced to a simple beam with fixed-fixed end conditions and an applied moment in the center $M_0 = Pe$. The maximum bending moment for this case can be found [3] as

$$M_{max} = \frac{M_0}{2} = \frac{Pe}{2} .$$

Now, the maximum tensile stress can be found by summing the contributions from the tensile load, P, and the bending moment, M_0.

$$\sigma_{total} = \sigma_{tensile} + \sigma_{bending} .$$

Consider a unit length of weld. Then

$$\sigma_{tensile} = \frac{P}{t \times 1} = \frac{P}{t},$$

and

$$\sigma_{bending} = \frac{6M_0}{t^2}$$

so

$$\sigma_{total} = \frac{P}{t} + \frac{6Pe/2}{t^2} = \frac{P}{t}\left[1 + 3\,\frac{e}{t}\right] = \sigma_{tensile} \times k_{offset} \; .$$

where $k_{offset} = 1 + 3e/t$. All data were converted using the full theoretical effect of weld offset.

2. Conversion to $R = -1$

The Goodman equation was used to convert mean and alternating stresses to equivalent $R = -1$ or pure alternating stresses ($R = \sigma_{min}/\sigma_{max}$). The equation for the modified Goodman line [4] is

$$\sigma_{alt} = \sigma_e - \left(\frac{\sigma_e}{\sigma_{ult}}\right)\sigma_{mean}$$

but $\sigma_e = \sigma_{R=-1}$, therefore

$$\sigma_{R=-1} = \frac{\sigma_{alt}}{1 - \frac{\sigma_{mean}}{\sigma_{ult}}}$$

For example, for specimen 9.1, $\sigma_{mean} = 141$ ksi, $\sigma_{alt} = 15.7$ ksi. From tensile test data, $\sigma_{ult} = 199$ ksi. Therefore,

$$\sigma_{R=-1} = \frac{15.7}{1 - \frac{141}{199}} = 53.9 \text{ ksi} \; .$$

3. Offset Correction and Conversion to $R = -1$ Combined

The "corrected" stress that is plotted in figure 3 is calculated by first considering the stress-raising effect of weld offset and then converting the resulting mean and alternating stress to an equivalent $R = -1$ stress using the Goodman relation as shown above. It is assumed that loads redistribute in the case where calculated surface stresses are above yield due to the weld offset. Thus, for $\sigma_{mean,corr} + \sigma_{alt,corr} > \sigma_y$, the value $\sigma_{mean,corr} = \sigma_y - \sigma_{alt,corr}$ is substituted for the corrected mean stress while the alternating stress is left unaltered.

For example, for specimen 9-3 the nominal mean stress, $\sigma_{mean,nom} = 136.1$ ksi and the nominal alternating stress, $\sigma_{alt,nom} = 15.12$ ksi. From tensile test data, $\sigma_y = 177$ ksi. Now, $k_{offset} = 1 + 3(0.35) = 2.05$, thus

$$\sigma_{alt.corr} = 31.00 \text{ ksi}$$

and

$$\sigma_{mean.corr} + \sigma_{alt.corr} = 310.0 \text{ ksi} > \sigma_y \ .$$

so we substitute

$$\sigma_{mean.corr} = 177 - 30.0 = 147 \text{ ksi} \ .$$

and convert to $R = -1$ as described above:

$$\sigma_{R=-1} = \frac{31.0}{1 - \frac{147}{199}} = 116.6 \text{ ksi} \ .$$

REFERENCES

1. Memorandum from Robert Brunair, Sverdrup Technology, Inc., to Karen Spanyer, ED25 NASA MSFC: Reponse to TD No. 611-003, June 6, 1990.

2. Rocketdyne Internal Letter MPR-88-0644.

3. "Roark's Formulas for Stress and Strain," 6th edition, p. 107.

4. Shigley, E.S., and Mitchell, L.D.: "Mechanical Engineering Design," 4th edition, McGraw-Hill, New York, New York, 1983.

APPROVAL

THE EFFECT OF WELD POROSITY ON THE CRYOGENIC FATIGUE STRENGTH OF ELI GRADE Ti-5A1-2.5Sn

By P.R. Rogers, R.C. Lambdin, and D.E. Fox

The information in this report has been reviewed for technical content. Review of any information concerning Department of Defense or nuclear energy activities or programs has been made by the MSFC Security Classification Officer. This report, in its entirety, has been determined to be unclassified.

Paul H. Schuerer

PAUL H SCHUERER
Director, Materials and Processes Laboratory

☆ U.S. GOVERNMENT PRINTING OFFICE 1992–631-060/60184